New Multifunctional Poly(lactide acid) Composites: Mechanical, Antibacterial, and Degradation Properties

E. Fortunati,[1] I. Armentano,[1] A. Iannoni,[1] M. Barbale,[2] S. Zaccheo,[2] M. Scavone,[3] L. Visai,[3,4,5] J. M. Kenny[1,6]

[1]*Materials Engineering Centre, UdR INSTM, NIPLAB, University of Perugia, Terni, Italy*
[2]*Novamont S.p.A., Novara, Terni, Italy*
[3]*Molecular Medicine Department University of Pavia, Viale Taramelli 3/b and Center for Tissue Engineering (CIT), University of Pavia, Via Ferrata 1, Pavia 27100, Italy*
[4]*Fondazione S. Maugeri, IRCCS, Istituto Scientifico di Pavia, Via S. Maugeri, 4, Pavia 27100, Italy*
[5]*International Centre for Studies and Research in Biomedicine (I.C.B.), 16 a, Bd. de la Foire, L-2015 Luxembourg*
[6]*Institute of Polymer Science and Technology, CSIC, Juan de la Cierva 3, Madrid 28006, Spain*

Received 4 March 2011; accepted 1 June 2011
DOI 10.1002/app.35039
Published online 3 October 2011 in Wiley Online Library (wileyonlinelibrary.com).

ABSTRACT: The aim of this work was to study the effect of the innovative combination of microcrystalline cellulose (MCC) and silver nanoparticles (Ag) on the poly (lactide acid) (PLA) composite properties, to modulate the PLA mechanical response and induce an antibacterial effect. The preparation and characterization of PLA-based composites with MCC and Ag nanoparticles by twin-screw extrusion followed by injection molding is reported. A film procedure was also performed to obtain PLA and PLA composite films with a thickness ranged between 20 and 60 μm. The analysis of disintegrability in composting conditions by means of visual, morphological, thermal, and chemical investigations was done to gain insights into the post-use degradation processes. Tensile test demonstrated the MCC reinforcing effect, while a bactericidal activity of silver-based composites against a Gram-negative bacteria (*Escherichia coli*) and a Gram-positive bacteria (*Staphylococcus aureus*) was detected at any time points and temperatures analyzed. Moreover, the disintegrability in composting showed that MCC is able to promote the degradation process. The combination of MCC and Ag nanoparticles in PLA polymer matrix offers promising perspectives to realize multifunctional ternary composites with good mechanical response and antibacterial effect, maintaining the optical transparency and the disintegrability, hence suitable for packaging applications. © 2011 Wiley Periodicals, Inc. J Appl Polym Sci 124: 87–98, 2012

Key words: biodegradable; composites; compounding; degradation; nanoparticle

INTRODUCTION

Biodegradable polymers have attracted great scientific and technological interest world wide because they have a well-grounded role in reducing the polymer waste problem.[1] In the family of biodegradable synthetic polymers, poly(lactide acid) (PLA) appears one of the most attractive for applications in agriculture and as packaging material[2] for its bio/hydro-degradability and the biorenewable profile.[3,4] PLA is a thermoplastic polyester, derived from the fermentation of starch and other polysaccharide sources[5] and it is becoming increasingly popular due to its high mechanical strength and easy processability compared with other biopolymers. Moreover, PLA is naturally degraded in soil or compost[6–8] and the resulting degradation products are totally assimilated by microorganisms such as fungi or bacteria.[2] However, PLA has lower water vapour permeability, poor mechanical and thermal properties, and limited barrier properties compared with equivalent petroleum based polymers.[9] The preparation of micro- and nano-composites represents a promising method to improve the physical properties of biopolymers, without affecting the transparency.[10–12] Microcrystalline cellulose (MCC) is used as a highly effective additive to improve the properties of polymer in several application fields.[13]

Demand for safe, minimally processed, food products presents major challenges to the food-packaging industry to develop packaging concepts for maintaining the safety and quality of products. In this contest, the active food-packaging concepts provide some additional functions in comparison with traditional passive materials that are limited to protection of the food product against external influences.

Correspondence to: I. Armentano (ilaria.armentano@unipg.it).

Contract grant sponsor: INSTM.
Contract grant sponsor: Regione Umbria and Italian Ministry of Education, University, and Research coordinated by Novamont; contract grant number: DM43839 (to S. Z.).

Active-packaging materials change the condition of the packaged product to extend shelf-life, improve microbial food safety, and/or improve sensorial properties. Antimicrobial active-packaging attracts more and more attention from the food and packaging industry, because of an increasing consumer demand for minimally processed, preservative-free products.[14,15] The research interest in this field of material science stems from the fact that there are different methods to incorporate silver in various polymeric substrates. One conventional approach is by the deposition of metallic silver directly onto the surface of the substrate,[16–19] whereas an other approach to obtain antimicrobial polymer composites is by the incorporation of silver into molten polymers.[20,21] Nowadays, the introduction of new silver-based antimicrobial polymers represents a great challenge in packaging field because these composite systems combine the excellent high temperature processibility of the thermoplastics with the inherent antimicrobial property of the silver. They capture much attention not only because of the nontoxicity of the active Ag^+ to human cells[22] but also because of their novelty being a long lasting biocide with high temperature stability and low volatility. In Japan, silver-substituted zeolite has been developed as the most common antimicrobial agent incorporated into plastics while on June 9, 2000, the AgION™ Silver Ion Technology received the approval of the food and drug administration for use in all types of food-contact polymers in USA market.[23] The EU-wide regulatory instruments covering antimicrobial substances differ distinctively in scope, depending on both the intended application and the actual effect of the active substances. So far, it is not the active product itself, but its use conditions that determine which directive applies in regulating the marketing of food-packaging products with antimicrobial activity in the European Union.[23]

The effect of additives on the biodegradation of PLA has attracted great interest recently.[24] It is already assessed that PLA formulations require severe degradation conditions (as those provided by composting systems) to biodegrade in times compatible with useful post use elimination strategies.[25,26] In a previous work,[27] we reported the preparation and characterization of PLA-based composites, observing an increase of the thermomechanical and barrier properties of the different systems, with respect to the neat polymer. In this research, we studied in details the mechanical, antibacterial, and degradation in composting condition properties of PLA and its composites prepared with an innovative combination of MCC and Ag nanoparticles, to demonstrate the prospective approach offered by these new systems.

EXPERIMENTAL PART

Materials

Poly(lactide acid) (PLA) 3051D, with a specific gravity of 1.25 g/cm^3, a molecular weight (M_n) of ca. 1.42×10^4 g/mol, a melt flow index of 7.75 g/10 min (210°C, 2.16 kg) was supplied by Nature Works®, Minnetonka, MN. PLA pellets were dried in a vacuum oven at 98°C for 3 h. Commercial silver nanoparticles (Ag), P203, purchased by Cima Nano-Tech (Corporate Headquarters Saint Paul, MN), with a size distribution ranged from 20 to 80 nm, were thermal treated at 700°C for 1 h.[27] MCC (dimensions of 10–15 μm) was supplied by Sigma–Aldrich and dried under vacuum at 100°C for 1 h to remove absorbed water.

PLA composite processing

PLA composites were manufactured by using a twin-screw microextruder (Dsm Explore 5&15 CC Micro Compounder). Screw speed of 150 rpm and mixing time of 3 min were used to optimize material final properties. PLA pellets (10 g) and the reinforcement phases were put in the microextruder manually to reach a head force of 2500*N* while a temperature profile (three temperature steps:170–195–205°C) with a maximum temperature of 205°C was chosen for the mixing process, according to our previous study.[27] After the mixing, samples with 1 wt % of Ag nanoparticles and with 5 wt % of MCC were prepared by means of a DSM Xplore 10-mL injection molding machine to obtain ISO 527-2/5A tensile dog-bone bars. The injection pressure was set to 15 bar and the temperature maintained at 205°C. Binary bulk systems containing 1 wt % of silver nanoparticles or 5 wt % of MCC were produced and characterized and corresponding samples were named PLA/1Ag and PLA/5MCC. In the ternary bulk systems (PLA/5MCC/1Ag), 5 wt % of MCC were mixed with 1 wt % Ag nanoparticles in the PLA polymer matrix.

A film procedure was also performed to obtain PLA and PLA composite films with a thickness ranged between 20 and 60 μm. The preparation and characterization of neat PLA (PLA_film), binary (PLA/1Ag_film, PLA/5MCC_film), and ternary (PLA/5MCC/1Ag_film) systems have been previously reported.[27]

Characterization methods

PLA and PLA composites cross-section performed in liquid nitrogen were investigated by field emission scanning electron microscopy (FESEM, Supra 25-Zeiss), after gold sputtering, (sputtering conditions: 20 mA for 40 s at 0.08 bar, by using an AGAR, Auto Sputter Coater).

Sample mechanical behavior was evaluated by failure tensile test of dog-bone-shaped specimens (2-mm thick) using a digital Lloyd instrument LR 30K on the basis of UNI ISO 527 with a cross-head speed of 1 mm/min and a load cell of 30 kN. The data are expressed as mean value ± mean standard deviation of at least five measurements.

Disintegrability in composting conditions

Disintegrability of PLA and PLA composites was observed by means of a disintegration test in composting conditions according to the ISO 20200 standard. A specific quantity of compost, supplied by Gesenu S.p.a., was mixed together with the synthetic biowaste, prepared with certain amount of sawdust, rabbit food, starch, sugar, oil, and urea. The water content of the substrate was around 50 wt % and the aerobic conditions were guaranteed by mixing it softly. The injection molded samples cut to have approximately $15 \times 5 \times 2$ mm^3 specimens were then buried at 4–6 cm depth in perforated boxes, containing the prepared mix, and incubated at 58°C.[28,29] The samples were recovered at different disintegration steps, washed with distilled water, dried in oven at 37°C for 24 h, and weighed. The disintegrability value was obtained normalizing the sample weight, at different stages of incubation, to the initial ones. Surface microstructure of PLA and PLA composites at 7 and 14 days of incubation in composting was investigated by field emission scanning electron microscopy. Photographs of the samples were taken for visual comparison. Differential scanning calorimeter (DSC, Mettler Toledo 822/e) measurements were performed in the temperature range from −25 to 250°C, at 10°C/min, performing continuously two heating and one cooling scans. Melting temperature (T_m) and cold crystallization temperature (T_{cc}), determined as the maximum of the endothermic and exothermic signal, respectively, and the melting and cold crystallization enthalpies (ΔH_m, ΔH_{cc}) were determined from the first and second heating scan. Glass transition temperatures (T_g) were obtained from the first and second heating thermogram, using the midpoint between intersections of two parallel baselines, before and after the transition temperature. Thermogravimetric analysis (TGA, Seiko Exstar 6000) was performed on 10 mg weight samples, in nitrogen flow (250 mL/min), from 30 to 900°C at 10°C/min heating rate. Fourier infrared spectra of the samples in the 400–4000 cm^{-1} range were recorded by a Jasco FT-IR 615 spectrometer, in attenuated total reflection (ATR) mode.

The disintegration test in composting conditions was also performed on $30 \times 30 \times 0.02$ mm^3 films, for comparison with bulk materials. PLA and PLA composite film visual evaluation is presented in this article.

Antibacterial activity

The microorganisms used in this study were *Escherichia coli* RB (*E. coli* RB), provided by Dr. Roldano Bragoni (Zooprofilattico Institute of Pavia, Italy), and *Staphylococcus aureus* 8325-4 (*S. aureus* 8325-4), a gift from Timothy J. Foster (Department of Microbiology, Dublin, Ireland). *E. coli* RB was grown overnight in Luria Broth Bertani (LB) (Difco, Detroit, MI) and *S. aureus* 8325-4 in brain heart infusion (BHI) (Difco) under aerobic conditions at 37°C using a shaker incubator (New Brunswick Scientific, Edison, NJ). These cultures, used as source for the experiments, were reduced at a final density of 1×10^{10} cells/mL as determined by comparing the optical density at 600 nm (OD_{600}) of the sample with a standard curve relating OD_{600} to the cell number. To evaluate the antimicrobial activity of PLA and PLA composite films, 100 μL (1×10^4) of an overnight diluted cell suspension of *E. coli* or *S. aureus* was added and incubated at different temperatures (37, 24, and 4°C). Wells were used as controls. At the end of each incubation time (3 h and 24 h), the bacterial suspension was serially diluted and plated on the LB (*E. coli*) or BHI (*S. aureus*) agar plates, respectively. Cell survival was expressed as percentage of the CFU of bacteria grown on the materials samples to CFU of bacteria grown into 24-well polystyrene culture plates.

RESULTS

Morphological and mechanical characterization of PLA composites

The fracture surfaces and the mechanical characterization of PLA and PLA composites are reported in Figure 1, to investigate the filler dispersion and to study the failure mechanisms. FESEM images show that neat PLA fracture surface appears flat without an evident smoothness, while composite surface is characterized by a visible roughness due to the filler dispersion. The PLA/5MCC and PLA/5MCC/1Ag systems show a uniform distribution of MCC and Ag nanoparticles, however, the MCC still remains as aggregates of crystalline fibrils. Higher magnification images show that MCC is present in flakes with a compact structure, and the evident voids around the MCC aggregates indicate a poor adhesion between the PLA and MCC.

Figure 1 shows tensile curves (a) and Young modulus (b) for PLA and PLA composites. Tensile stresses are lower for the composites compared with pure PLA, and a decrease of composite elongation at break respect to the neat matrix is detected, clearly evident for PLA/5MCC systems [Fig. 1(a)]. Moreover, a decrease in tensile strength of about 10 MPa for the MCC-based systems was measured. The

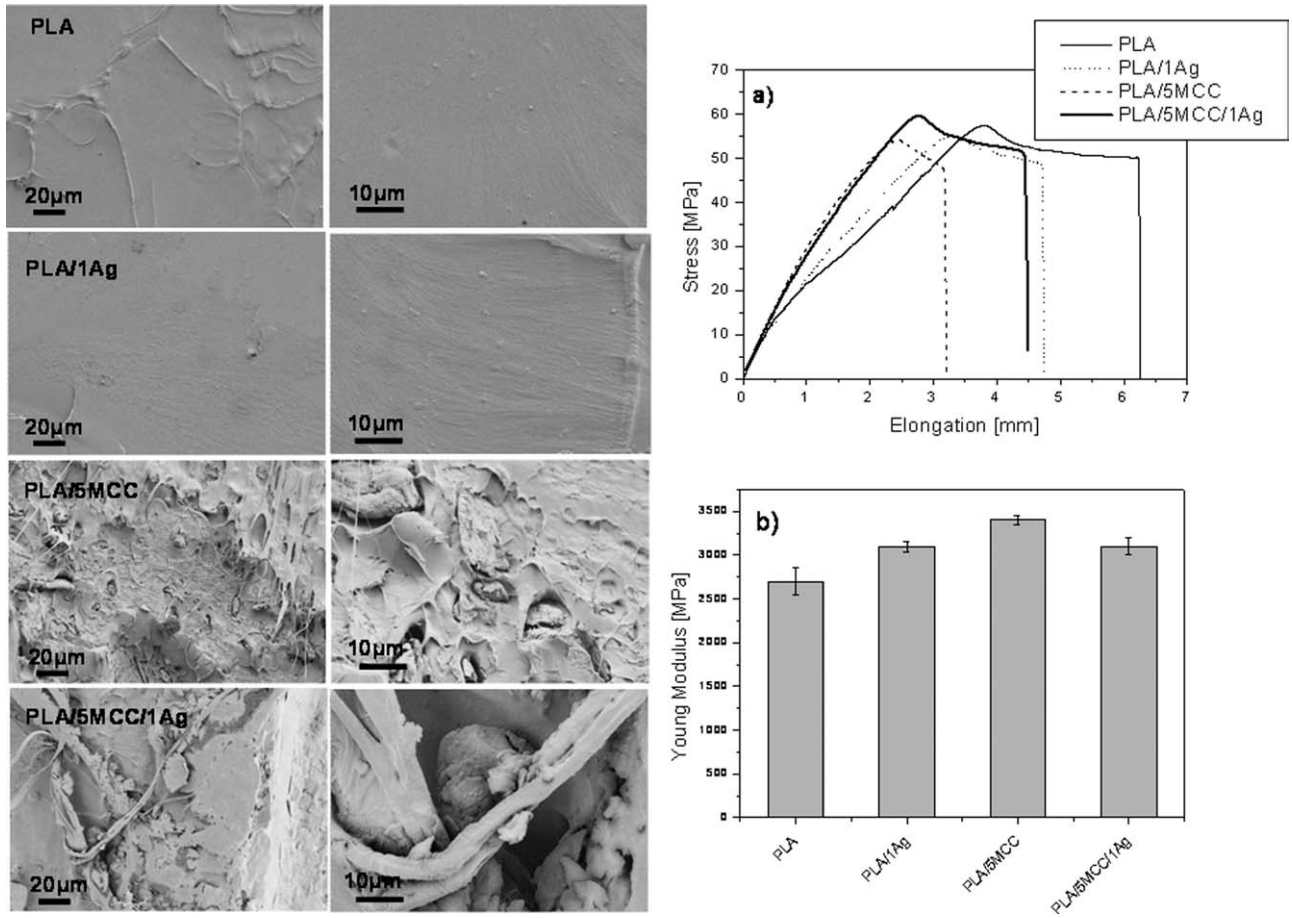

Figure 1 PLA and PLA composite fracture surface at different magnifications. Tensile curves (a) and Young modulus (b) for PLA and PLA composites.

lowering of elongation at break with the addition of fibres in the polymers is a common trend observed in thermoplastic composites in which the addition of stiff reinforcements causes stress concentrations.[30] Figure 1(b) shows that all composites have tensile modulus higher than neat PLA, and the PLA/5MCC system has the highest modulus with an increase of 26% respect to pure PLA highlighting the reinforcement effect exerted by MCC. However, in the case of PLA/5MCC/1Ag ternary system, a comparable modulus with respect to binary PLA/1Ag system (3.1 GPa) is detected.

The mechanical performance of composites is expected to depend on the following factors: (1) adhesion between the PLA matrix and cellulosic reinforcements, stress transfer efficiency of the interface; (2) volume fraction of the fibres; (3) aspect ratio of the reinforcements; (4) fiber orientation; and (5) crystallinity degree of the matrix.[31]

In our systems, MCC remains as crystalline fibril aggregates, and this could give an explanation for the low value of tensile stresses and elongation at break[10] compared with the polymer matrix.

Disintegrability in composting of PLA composites

Disintegrability in composting conditions was first evaluated by visual observation of the PLA and PLA composites. Figure 2 shows that all samples changed their colour and became opaque after 7 days of incubation, while they exhibited a considerable surface deformation and fractures starting from 14 days in composting. This effect at 14 days of incubation was more evident in the case of composites based on silver nanoparticles. The changes in sample colour could be a signal that the hydrolytic degradation process of the polymer matrix has started, thus inducing a change in the refraction index of the sample as a consequence of water absorption and/or presence of products formed by the hydrolytic process.[32,33] The disintegration test showed that materials were visibly disintegrated after 28 days, and PLA/5MCC was still present at 35 days. The Ag-based composites resulted to have the more evident effects of disintegration (Fig. 2). This result is confirmed by FESEM observations (Fig. 3): at 7 days of incubation PLA/1Ag shows deep fractures on the surface more evident than in the other composites. After 14 days of incubation, all systems are visibly

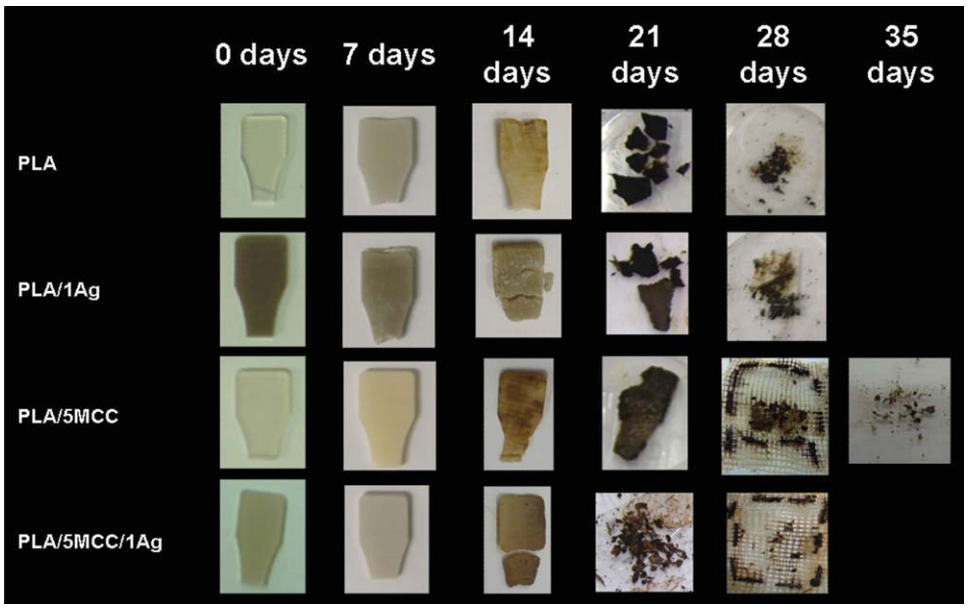

Figure 2 PLA and PLA composites before (0 days) and after different stages of disintegration in composting at 58°C. [Color figure can be viewed in the online issue, which is available at wileyonlinelibrary.com.]

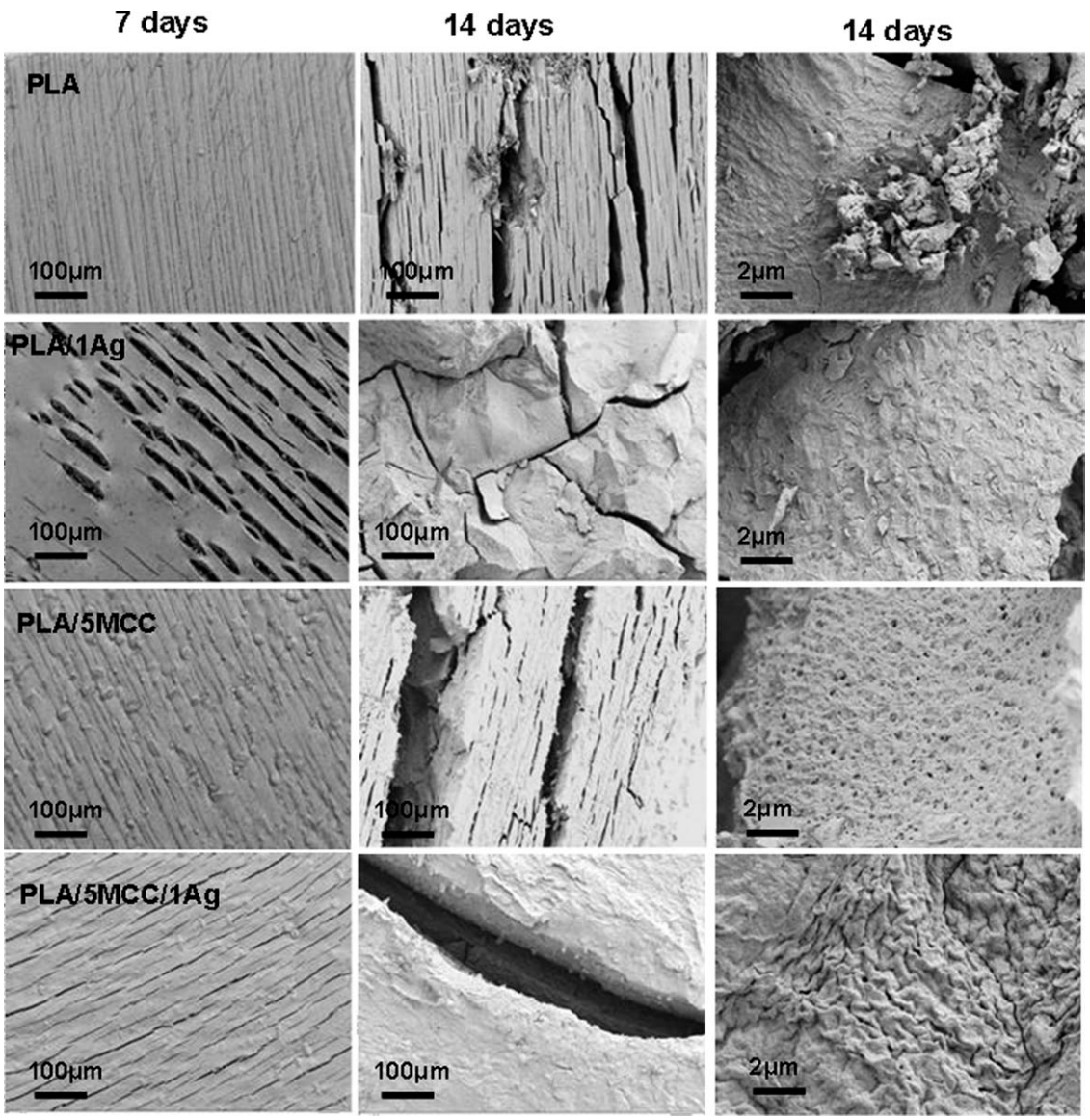

Figure 3 FESEM images of PLA and PLA composite surfaces after disintegration in composting at 58°C.

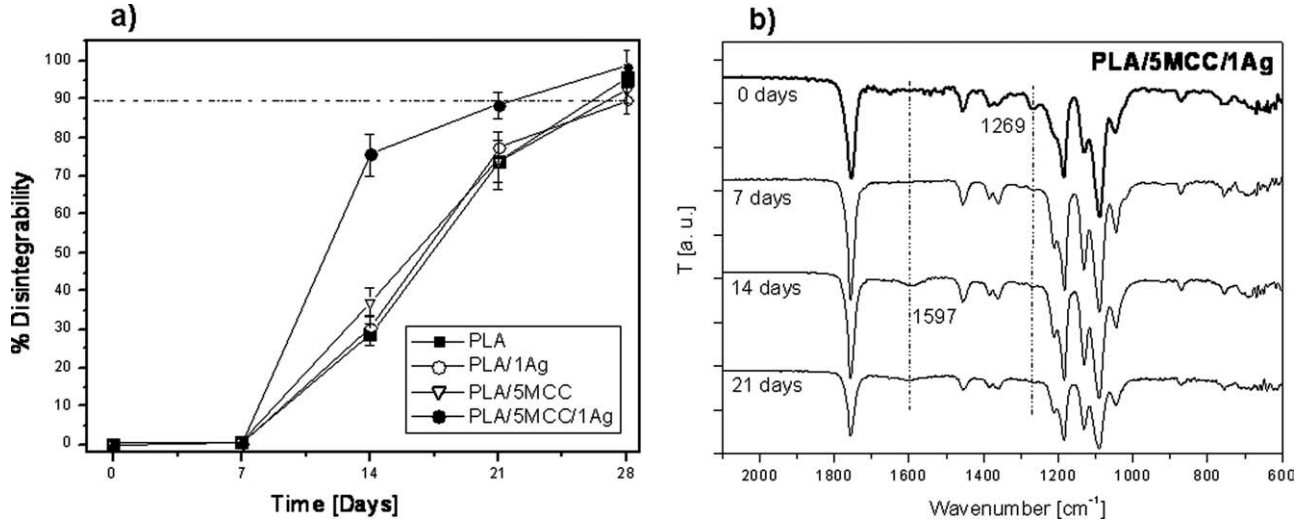

Figure 4 Disintegrability percentage values of PLA and PLA composites at different stages of incubation in composting. The line at 90% represents the goal of disintegrability test as reported in the ISO 20200 (a). Infrared spectra of PLA/5MCC/1Ag samples before and after different stages of disintegration in composting (b).

fractured, and fissures of 100 μm appear on the surface of MCC-based systems, in particular in the PLA/5MCC/1Ag ternary composite. This result is confirmed by disintegrability values [Fig. 4(a)] that remain constant for all systems until 7 days of incubation, while it reaches 30% at 14 days and then 70% at 21 days for neat PLA and binary systems. A different behavior is detected for PLA/5MCC/1Ag ternary sample that showed the highest rate of disintegration, namely 75% in 14 days and 88% in 21 days. It was reported that PLA degradation occurred in 2 weeks and was marked by the embrittlement of the samples.[10] During the initial phases of the disintegration, the high-molecular weight PLA chains are hydrolyzed to form lower molecular weight chains and this reaction can be accelerated by the presence of acids or bases.[34] In this case, Ag ion release, could acted as catalytic agents accelerating the disintegration process. The faster appearance of visual signs of degradation in composites and the more evident percentage of disintegration of PLA/5MCC/1Ag system at 14 days is likely to be due to the presence of hydroxyl groups belonging to the microcrystalline structure that plays a catalytic role on hydrolysis of the ester groups of the PLA.[8]

Chemical analysis (FTIR)

Figure 4(b) shows the FTIR spectra in the 2000–600 cm^{-1} range, of ternary composites before and after different degradation times in composting. The IR spectra of PLA composites display the typical stretching of carbonyl group (—C=O) at 1750 cm^{-1} by lactide, and the —C—O— bond stretching in —CH—O— group of PLA at 1182 cm^{-1}.[35] The change at 21 days of degradation in compositing is the appearance of the band at 1600 cm^{-1} corresponding to carboxylate ions in spectrum of degraded PLA composites, while the band at 1260 cm^{-1} corresponding to —C—O— stretch almost disappears in the spectrum of the degraded samples. The formation of carboxylate ions is due to microorganisms, which consume lactic acid and its oligomers on the surface and leave carboxylate ions at the chain end.[36] No significant difference is revealed between the PLA and PLA composites, during incubation in composting conditions.

Thermal analysis

Figure 5 shows the DSC thermograms of the first [Fig. 5(a,c)] and second [Fig. 5(b,d)] heating scan for PLA and PLA/5MCC/1Ag composites. The first heating thermograms, before the disintegration in composting, displayed successively the glass transition temperature (T_g), the cold crystallization exotherm (T_{cc}), and the melting endotherm (T_m). Cold crystallization for PLA matrix and PLA/5MCC/1Ag gives a crystalline phase which shows one endothermal peak in the first and second heating curves. The T_g was about 58°C, all curves had the T_{cc} at about 125°C, and the T_m at about 150°C (Table I). After 7 days of incubation, the cold crystallization temperature of all samples is not clearly visible in the first heating scan. Moreover, this effect is accompanied by the formation of a low temperature additional endothermic shoulder on melting (T_m'). The presence of multiple melting peaks in PLA could be related to the formation of different crystal structures[37] or to lamellar populations with different perfection

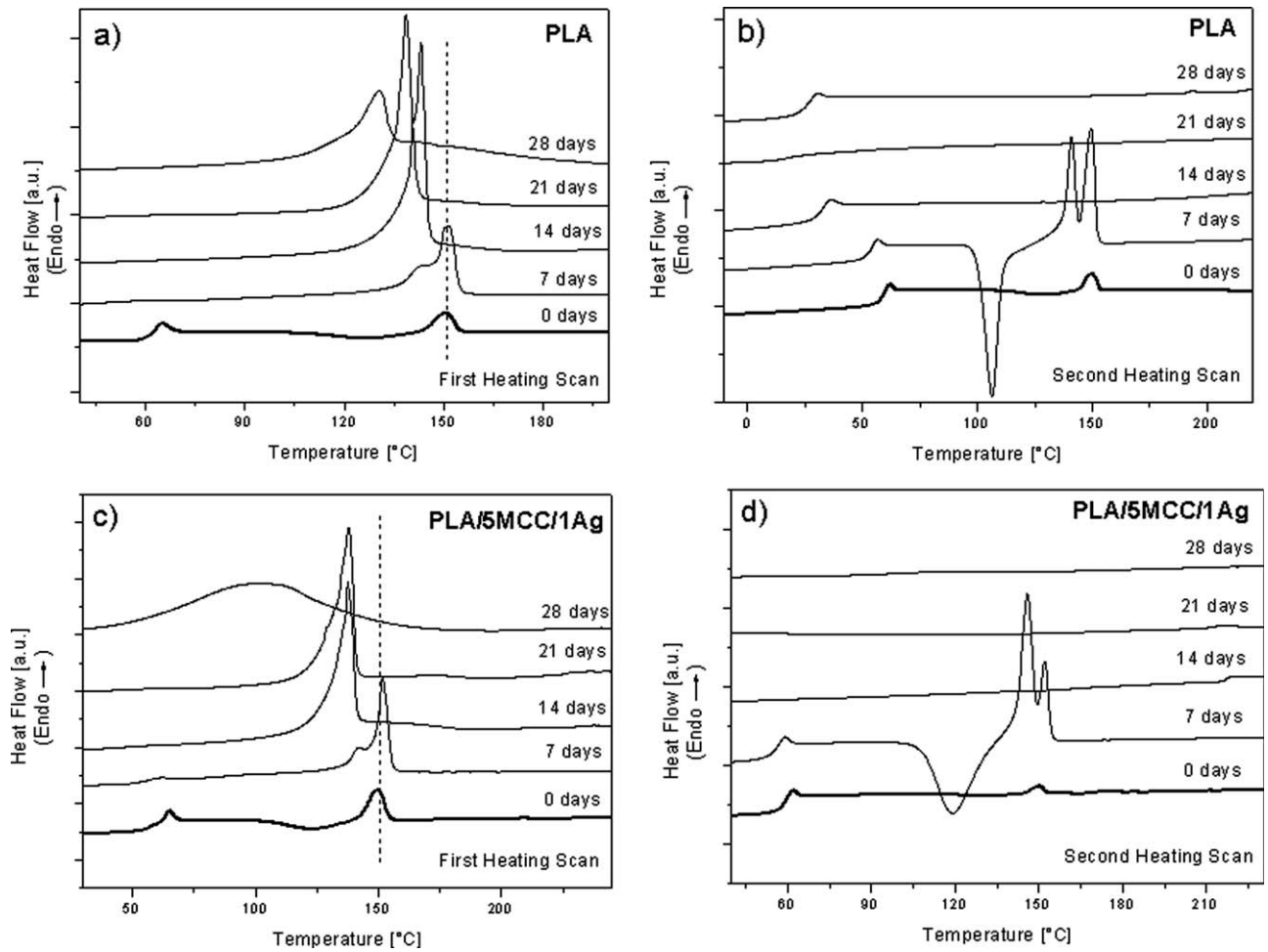

Figure 5 DSC thermograms of PLA (a, b) and PLA/5MCC/1Ag ternary composites (c, d) before and after different stages of disintegration in composting at 58°C.

degrees.[38,39] This phenomenon is more evident in the second heating scan [Fig. 5(b,d) and Table I] in which, on the seventh day of degradation, the presence of exothermic peak and the additional melting shoulder at low temperature are evident. After 7 days of degradation, cold crystallization and melting temperatures decrease with respect to their initial values as a consequence of a molecular chain degradation in composting according to the first heating scan [Fig. 5(a,c)] and to morphological observations. For all samples, the decrease of transition temperatures was evident, however, no big changes in these values were detected for the different systems. The first heating scan after 21 days in composting shows only the T_m whereas at the second heating, only the glass transition is evident, highlighting the degradation progress and the completely amorphous nature of the material, more clear in PLA/5MCC/1Ag composite [Fig. 5(c)]. A decrease of the T_g values, detected at the second heating scan, of about 10°C at 7 days and of about 28°C at 14 days of incubation for PLA and PLA composites [Fig. 5(b,d)] implies a probably increase in the polymer chain mobility due to a plasticizing effect of lactic acid oligomers formed on degradation.[40,41] Melting and cold crystallization enthalpies for the first and second heating scan, during the disintegrability in compositing conditions were reported in Table I. ΔH_m values increase with the degradation time for PLA and PLA composites, as consequence of the incubation temperature (58°C) and the disintegrability process.

DTG curves and the maximum degradation temperatures (T_{max}) of PLA and PLA composites before and at different times in composting are shown in Figure 6(a,b). A complete weight loss in a single step with a maximum at 357°C was detected for neat PLA and a similar behavior was found after degradation in composting [Fig. 6(a)]. However, a shift to lower degradation temperatures of about 19% in PLA was observed at 14 days of incubation, and the highest reduction was detected for the PLA/5MCC/1Ag ternary composite with a decrease in T_{max} of about 21% at 14 days and 25% after 28 days [Fig. 6(b)]. This result is in agreement with DSC analysis.

TABLE I
DSC Data of PLA and PLA Composites, First and Second Heating Scan

	First heating									
	0 days					7 days				
Samples	ΔH_{cc}	ΔH_m	T_{cc} (°C)	T_m' (°C)	T_m (°C)	ΔH_{cc}	ΔH_m	T_{cc} (°C)	T_m' (°C)	T_m (°C)
PLA	6.9 ± 0.4	9.8 ± 0.8	126.0 ± 0.2	–	150.3 ± 0.1	–	46.6 ± 1.0	–	145.1 ± 0.8	150.1 ± 1.0
PLA/1Ag	7.2 ± 0.1	12.6 ± 1.0	124.8 ± 0.4	–	150.5 ± 0.3	–	32.1 ± 0.8	–	145.7 ± 0.1	151.3 ± 0.6
PLA/5MCC	14.9 ± 0.9	21.7 ± 0.7	122.2 ± 0.2	–	150.1 ± 0.1	–	32.8 ± 0.2	–	147.1 ± 0.4	151.0 ± 0.4
PLA/5MCC/1Ag	9.5 ± 0.3	14.0 ± 0.6	123.4 ± 0.8	–	150.0 ± 0.4	–	38.2 ± 1.0	–	148.0 ± 0.4	151.8 ± 0.1
	14 days					21 days				
	ΔH_{cc}	ΔH_m	T_{cc} (°C)	T_m' (°C)	T_m (°C)	ΔH_{cc}	ΔH_m	T_{cc} (°C)	T_m' (°C)	T_m (°C)
PLA	–	78.1 ± 0.4	–	140.3 ± 1.0	143.1 ± 0.1	–	72.6 ± 2.0	–	139.3 ± 0.9	142.7 ± 0.8
PLA/1Ag	–	66.7 ± 1.0	–	140.6 ± 0.5	144.6 ± 0.5	–	95.8 ± 1.0	–	139.6 ± 0.8	143.7 ± 0.9
PLA/5MCC	–	70.5 ± 1.0	–	136.4 ± 0.7	140.2 ± 0.3	–	87.1 ± 2.0	–	138.0 ± 1.0	–
PLA/5MCC/1Ag	–	57.9 ± 1.0	–	135.3 ± 1.0	139.3 ± 0.8	–	81.6 ± 2.0	–	139.2 ± 1.0	–
	Second heating									
	0 days					7 days				
	ΔH_{cc}	ΔH_m	T_{cc} (°C)	T_m (°C)		ΔH_{cc}	ΔH_m	T_{cc} (°C)	T_m' (°C)	T_m (°C)
PLA	2.4 ± 0.3	3.9 ± 0.3	128.3 ± 0.3	149.5 ± 0.1		32.4 ± 2.0	43.9 ± 2.0	99.1 ± 1.0	134.7 ± 2.0	143.1 ± 2.0
PLA/1Ag	2.6 ± 0.4	3.8 ± 0.8	128.7 ± 0.9	149.0 ± 0.1		32.8 ± 0.3	42.0 ± 0.3	106.0 ± 1.0	142.6 ± 0.3	148.4 ± 0.2
PLA/5MCC	6.8 ± 0.9	10.9 ± 1.0	126.4 ± 0.7	149.7 ± 0.4		32.2 ± 0.4	42.6 ± 0.1	100.7 ± 1.0	141.5 ± 2.0	148.1 ± 2.0
PLA/5MCC/1Ag	3.2 ± 0.7	4.2 ± 0.8	127.8 ± 1.0	149.7 ± 0.2		28.0 ± 2.0	38.4 ± 2.0	118.1 ± 0.8	145.6 ± 0.2	149.0 ± 0.3

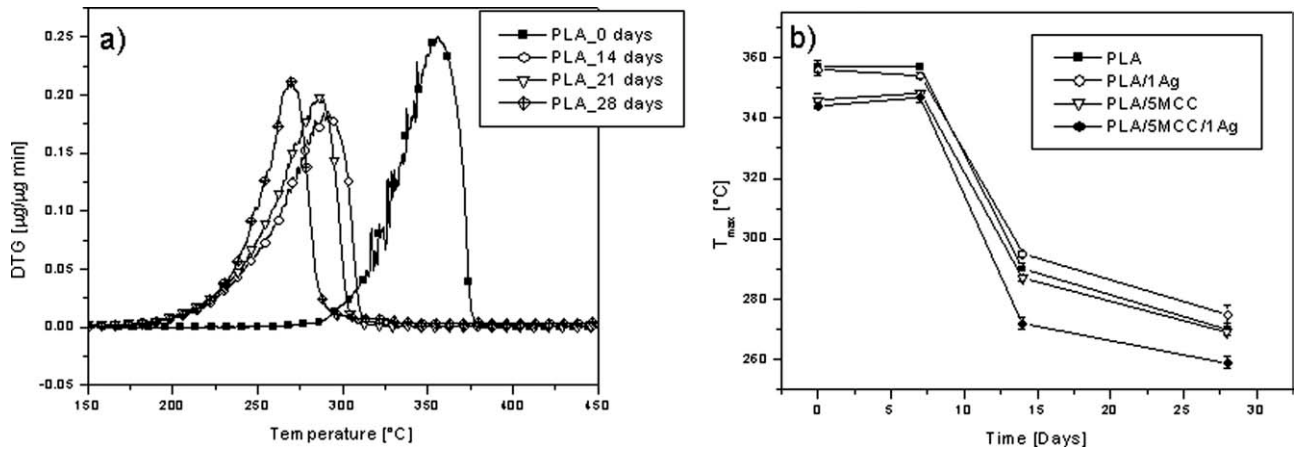

Figure 6 DTG curves for PLA at different stages of disintegration (a) and T_{max} values of PLA and composite systems (b) before and after the disintegrability in composting at 58°C.

TABLE II
Mechanical Properties of PLA and PLA Composite Films

Samples	σ_Y (MPa)	ε_Y (%)	σ_b (MPa)	ε_b (%)	E_{YOUNG} (MPa)
PLA_film	54 ± 5	2.2 ± 0.5	43 ± 5	90 ± 10	2400 ± 100
PLA/1Ag_film	31 ± 3	2.1 ± 0.5	22 ± 3	11 ± 2	2500 ± 50
PLA/5MCC_film	36 ± 4	2.1 ± 0.2	28 ± 3	20 ± 2	2900 ± 100
PLA/5MCC/1Ag_film	23 ± 2	2.4 ± 0.3	22 ± 2	20 ± 2	2600 ± 100

PLA composite films

The production of PLA and PLA composite binary and ternary films appears to be a promising approach for packaging application. Films with a thickness ranged between 20 and 60 µm were produced and optical, mechanical, and antibacterial properties were mainly evaluated. Composite films do not show a significant reduction in the amount of light being transmitted (data do not shown).

Table II summarizes the mechanical properties of PLA and PLA composite films. PLA processed films have yield stress of 54 MPa, a tensile strength of 43

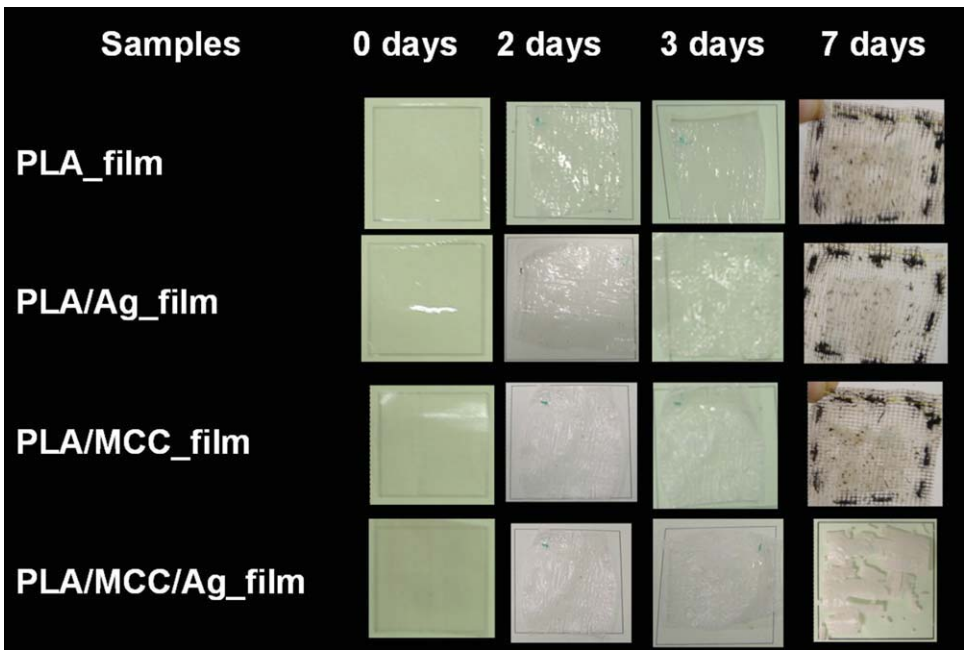

Figure 7 PLA and PLA composite films before (0 days) and after different stages of disintegration in composting at 58°C. [Color figure can be viewed in the online issue, which is available at wileyonlinelibrary.com.]

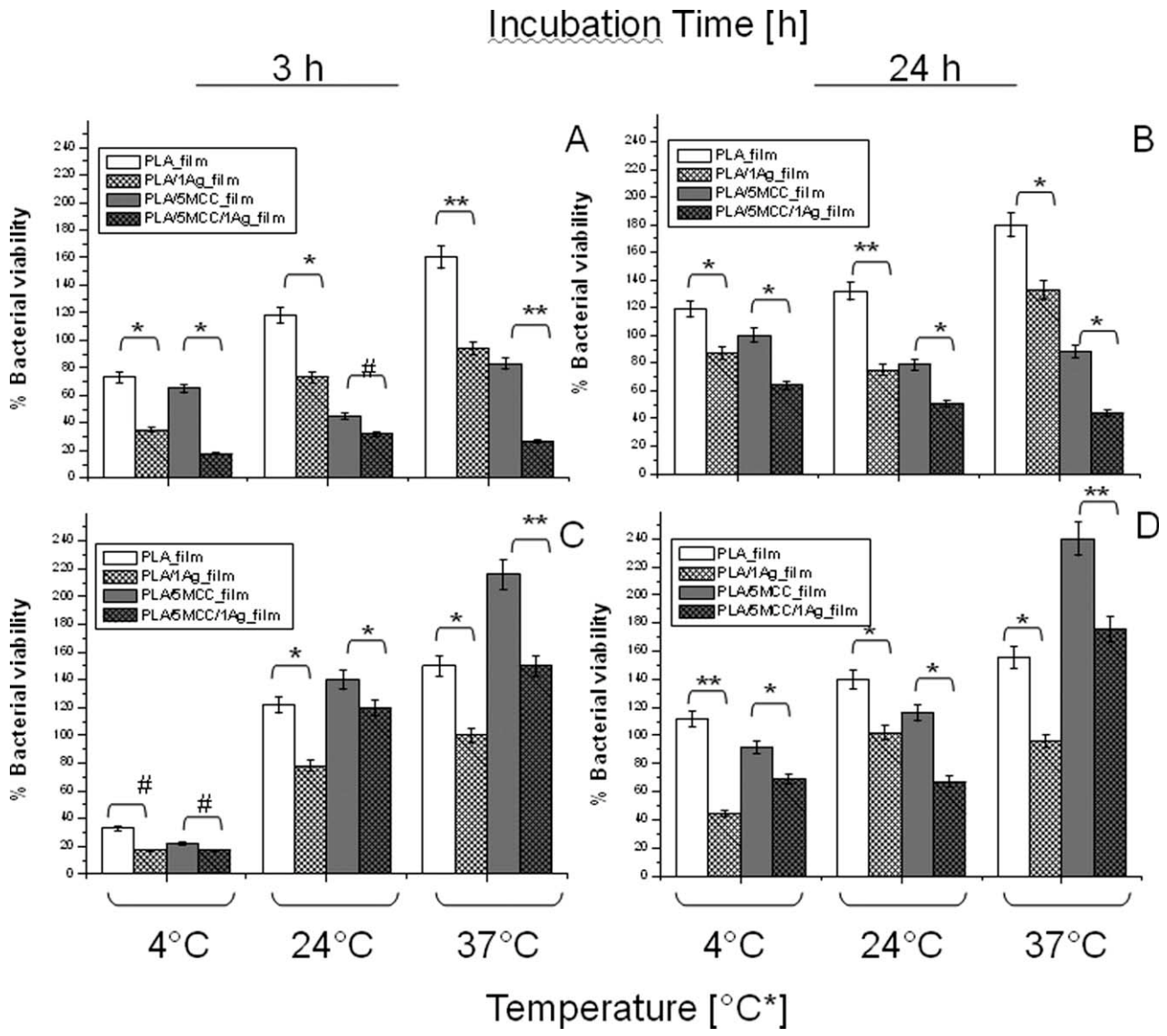

Figure 8 Antibacterial properties of new multifunctional PLA composites at different temperatures. *E. coli* RB (A, B) and *S. aureus* 8325-4 (C, D) cells were incubated on PLA and PLA composite films for 3 h and 24 h at 4, 24, and 37°C as reported in "Materials and Methods." Results are expressed on a biomaterial-basis and are presented as an average ± standard deviation (*$P < 0.05$; **$P < 0.01$; ***$P < 0.001$, #$P > 0.05$).

MPa and a very high deformation at break (90%) compared with the bulk systems. PLA composites show a decrease in tensile strength values of 15 MPa for PLA/5MCC_film and of about 21 MPa for the systems loaded with silver nanoparticles and also a lowering of elongation at break, as in the case of bulk systems, common in thermoplastic composite films[30] was detected. All composite films show Young modulus higher than pure PLA_film (2.4 GPa), and the PLA/5MCC_film system has the highest modulus (2.9 GPa),[27] following the same trend even of the bulk composites.

Disintegrability in composting

The disintegrability of PLA and PLA composite films in composting conditions was studied to evaluate the effect of the contact between the organic substrate and these films. Figure 7 shows that all the materials were visibly disintegrated after 7 days, especially the PLA/5MCC/1Ag_film ternary system that appears completely embrittled. Moreover, composites with MCC have the highest rate of disintegration in composting, confirming the results obtained for the bulk materials. These short degradation times of PLA films are probably due to high temperature and to the low thickness of the tested samples. The rate of hydrolytic degradation of PLA is, in fact, strongly dependent on temperature and the humidity level.[5,34] Further investigations, in accordance with other standards, allowed the study of disintegrability trend of the PLA and PLA composite films at lower incubation temperature.

Antibacterial properties

Figure 8 shows the viability of *S. aureus* (Panels A and B) and *E. coli* (Panels C and D) cells on PLA and PLA composite films incubated for 3 h and 24 h at 4, 24, or 37°C, respectively. In general, a significant difference in bacterial viability between PLA_film and PLA/1Ag_film ($P < 0.05$), PLA/5MCC_film and PLA/5MCC/1Ag_film ($P < 0.05$) was observed: PLA samples containing Ag nanoparticles showed a greater antibacterial activity against *E. coli* than *S. aureus* cells. These data are in agreement with previous results showing that silver ions interfering with the respiratory chain cause a decrease of the bacterial viability and those Ag nanoparticles are more toxic to *E. coli* than to *S. aureus*.[42–44] Furthermore, the reduction of *E. coli* survivability was more evident on PLA/5MCC/1Ag_film than on PLA/1Ag_film regardless of time and temperature (Fig. 8, Panels A and B). However, on *S. aureus* cells, the result was quite different: PLA/1Ag_film exhibited a greater antibacterial activity in comparison with PLA/5MCC/1Ag_film. As previously reported,[45] the electron-acceptor characteristic of *S. aureus* determines an higher binding of these bacterial cells to PLA/5MCC_film, therefore reducing the antibacterial efficacy of PLA/5MCC/1Ag_film. Furthermore, this effect was more marked at shorter (Fig. 8, Panel C) than at longer incubation times (Fig. 8, Panel D) regardless of the temperature. As clearly shown by our data, this adhesion property is not observed for *E. coli*. In summary, these data highlight the effectiveness of silver nanoparticles combined with MCC on the reduction of bacterial viability at different times and temperatures. The content of Ag nanoparticles (1 wt %) in the composites is able to determine an evident antimicrobial effect and provides an active-system for food-packaging applications. However, this low silver quantities does not influence the organic biowaste maturation process, the final parameters (e.g., pH, volatile solids, and ash) are in agreement with the ISO20200.

CONCLUSIONS

PLA-based composites, bulk and films, are successfully prepared combining MCC and Ag nanoparticles. Morphology studies revealed a well dispersion of silver nanoparticles and the presence of MCC aggregates, while the mechanical properties demonstrated the MCC reinforcing effect. The disintegrability in composting showed that MCC-based systems, bulk and films, have the highest rate of degradation in composting. A bactericidal effect of PLA/1Ag_film on *S. aureus* and PLA/5MCC/1Ag_film on *E. coli* was detected at any time points and temperatures analyzed. These systems may offer good perspective for food-packaging applications, which requires an antibacterial effect constant over time.

The Authors acknowledge Gesenu S.p.a. for compost supply and the International Centre for Studies and Research in Biomedicine (I.C.B.) in Luxembourg.

References

1. Yang, S. H.; Yoon, S. J.; Kim, N. M. Polym Degrad Stab 2005, 87, 131.
2. Liu, L.; Li, S.; Garreau, H.; Vert, M. Biomacromolecules 2000, 1, 350.
3. Kawashima, N.; Ogawa, S.; Obuchi, S.; Matsuno, M.; Yagi, T. Poly(Lactic Acid) "LACEA." Doi, Y., Steinbüchel, A., Eds. In Biopolymers in 10 Volumes; Weinheim: Wiley-VCH, 2002; Vol. 4, pp 251–274.
4. Vert, M. Poly(Lactic Acid). In Wnek, G. E., Bowlin, G. L., Eds. In Encyclopedia of Biomaterials and Biomedical Engineering; New York: Marcel Dekker, 2004; Vol. 2, pp 1254–1263.
5. Lunt, J. Polym Degrad Stab 1998, 59, 145.
6. Tsuji, H.; Mizuno, A.; Ikada, Y. J Appl Polym Sci 1998, 70, 2259.
7. Ghorpade, V. M.; Gennadios, A.; Hanna, M. A. Bioresource Technol 2001, 76, 57.
8. Fukushima, K.; Abbate, C.; Tabuani, D.; Gennari, M.; Camino, G. Polym Degrad Stab 2009, 94, 1646.
9. Petersen, K.; Nielsen, P.; Olsen, M. Starch 2001, 53, 356.
10. Mathew, A. P.; Oksman, K.; Sain, M. J Appl Polym Sci 2005, 97, 2014.
11. Bandyopadhyay, S.; Chen, R.; Giannelis, E. P. Polym Mater Sci Eng 1999, 81, 159.
12. Alexandra, M.; Dubois, P. Mater Sci Eng R 2000, 28, 1.
13. Ma, X.; Chang, P. R.; Yu, J. Carbohydr Polym 2008, 72, 369.
14. Vermeiren, L.; Devlieghere, F.; van Beest, M.; de Kruijf, N., Debevere, J. Trends Food Sci Technol 1999, 10, 77.
15. Collins-Thompson, D.; Hwang, C. A. Packaging with antimicrobial properties. In: Robinson, R. K.; Batt, C. A.; Patel, P. D., editors, Encyclopedia of food microbiology, Academic Press, London, UK (2000), pp. 416–420.
16. Saint, S.; Elmore, J. G.; Sullivan, S. D.; Emerson, S. S.; Koepsell, T. D. Am J Med 1998, 105, 236.
17. Dowling, D. P.; Betts, A. J.; Pope, C.; McConnell, M. L.; Eloy, R.; Arnaud, M. N. Surf Coat Technol 2003, 16, 637.
18. Gray, J. E.; Norton, P. R.; Marolda, C. L.; Valvano, M. A.; Griffiths, K. Biomaterials 2003, 24, 2759.
19. Klueh, U.; Wagner, V.; Kelly, S.; Johnson, A.; Bryers, J. D. J Biomed Mater Res 2000, 53, 621.
20. Saito, R., Okamura, S., Ishizu, K. Polymer 1993, 34, 1189.
21. Kumar, R., Munstedt, H. M. Biomaterials 2005, 26, 2081.
22. Williams, R. L.; Doherty, P. J.; Vince, D. G., Grashoff, G. J.; Williams, D. F. Crit Rev Biocompat 1989, 5, 221.
23. Quintavalla, S.; Vicini, L. Meat Sci 2002, 62, 373.
24. Russias, J.; Saiz, E.; Nalla, R. K.; Gryn, K.; Ritchie, R. O.; Tomsia, A. P. Mat Sci Eng C 2006, 26, 1289.
25. Navarro, M.; Ginebra, M. P.; Planell, J. A.; Barrias, C. C.; Barbosa, M. A. Acta Biomater 2005, 1, 411.
26. Shah, A. A.; Hasan, F.; Hameed, A.; Ahmed, S. Biotechnol Adv 2008, 26, 246.
27. Fortunati, E.; Armentano, I.; Iannoni, A.; Kenny, J. M. Polym Degrad Stab 2010, 95, 2200.
28. Hakkarainen, M.; Karlsson, S.; Albertsson, A. C. Polymer 2000, 41, 2331.
29. Kunioka, M.; Ninomiya, F.; Funabashi, M. Polym Degrad Stab 2006, 91, 1919.
30. Colom, X.; Carrasco, F.; Pages, P.; Canavate, J. Compos Sci Technol 2003, 63, 161.

31. Dufresne, A.; Dupeyre, D.; Paillet, M. J Appl Polym Sci 2003, 87, 1302.
32. Li, S.; Girard, A.; Garreau, H.; Vert, M. Polym Degrad Stab 2001, 71, 61.
33. Li, S.; McCarthy, S. Biomaterials 1999, 20, 35.
34. Ho, K. L. G.; Pometto, A. L.; Gadea, A.; Briceno, J. A.; Rojas, A. J Environ Polym Degrad 1999, 7, 173.
35. Chen, C.C.; Chueh, J. U.; Tseng, H.; Huang, H. M.; Lee, S. Y. Biomaterials 2003, 24, 1167.
36. Khabbaz, F.; Karlsson, S.; Albertsson, A. C. J Appl Polym Sci 2000, 78, 2369.
37. Yasuniwa, M.; Sakamo, K.; Ono, Y.; Kawahara, W. Polymer 2008, 49, 1943.
38. Kong, Y.; Hay, J. N. Polymer 2003, 44, 623.
39. Liu, T.; Petermann, J. Polymer 2001, 42, 6453.
40. Tsuji, H.; Tezuka, Y. Macromol Biosci 2005, 5, 135.
41. Tsuji, H.; Ikada, Y. J Appl Polym Sci 1997, 63, 855.
42. Rai, M.; Yadav, A.; Gade, A. Biotechnol Adv 2009, 27, 76.
43. Li, W. R.; Xie, X. B.; Shi, Q. S.; Duan, S. S.; Ouyang, Y. S.; Chen, Y. B. Biometals 2011, 24, 135.
44. Li, W. R.; Xie, X. B.; Shi, Q. S.; Zeng, H. Y.; Ou-Yang, Y. S.; Chen, Y. B. Appl Microbiol Biotechnol 2010, 85, 1115.
45. Prokopovich, P.; Perni, S. J Mater Sci Mater Med 2009, 20, 195.